Numerical Simulation of Dual-Mode Scramjet Combustor with Significant Upstream Interaction

Rahul Ingle, Directorate of Computational Dynamics, Defence Research and Development Laboratory, India

Debasis Chakraborty, Directorate of Computational Dynamics, Defence Research and Development Laboratory, India

ABSTRACT

This paper is concerned with a numerical study corresponding to experimental investigation of Chinzei and co-workers on hydrogen fueled dual-mode scramjet engine essentially to understand the key features of upstream interaction, mixing and combustion. Three dimensional Navier Stokes equations along with a K-∈ turbulence model and infinitely fast kinetics are solved using commercial CFD software. Reasonable agreement has been obtained between the computed surface pressure with experimental values and the results of other numerical simulations. Insights into the flow features inside the combustor are obtained through analysis of various thermochemical parameters. The comparison of surface pressure with experimental results and other numerical results demonstrated that simple kinetics and turbulence – chemistry interaction model may be adequate to address the overall flow features in the combustor. A principal conclusion is that the boundary layer at the combustor entry has a pronounced effect on the flow development in the dual-mode scramjet combustor and causes significant upstream interaction.

Keywords: *Dual Mode Scramjet Combustor, Hydron Fueled Dual-Mode Scramjet Engine, Numerical Simulation, Scramjet Combustor, Upstream Interaction*

1. INTRODUCTION

In recent years, a significant amount of high speed combustion research is directed towards understanding the complex flow phenomena inside a scramjet combustor over a range of operating conditions. Studies – analytical, experimental and numerical – are focused on different aspects of the flow field in the various components of scramjet engines viz., intake, combustor, nozzle etc. The components have also been coupled to make a complete scramjet engine, and the flow fields of the engine with different fuel injection systems have been subjected to numerical and experimental exploration. Curran (2001) reviewed comprehensively the status of scramjet engine in first 40 years

DOI: 10.4018/ijmmme.2012070105

Figure 1. Schematic of DMRJ operation

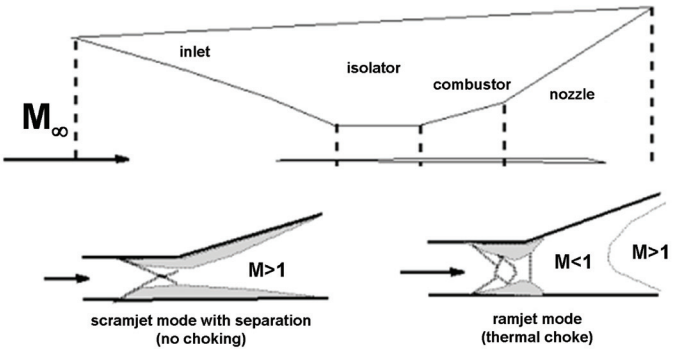

and identified two emerging scramjet applications namely (1) Hydrogen fueled scramjet engine to access space and (2) Hydrocarbon fueled scramjet engine for an air launched missile. To increase the flight envelope of the air breathing vehicle, Billig (1993) and Cockrell et al. (2002) introduced Dual-mode Ramjet Scramjet (DMRJ) concept which integrate the advantageous capabilities of both ramjets and scramjets into one flow path.

In a ramjet, the flow is subsonic by the time it gets to the combustor. In a scramjet, the flow remains supersonic through the combustor. The dual mode scramjet bridges the gap between the ramjet and scramjet. It uses the same combustor geometry for both the ramjet and scramjet modes, but operates with a thermal throat in ramjet mode. This combination may enable a vehicle to operate from Mach 3 to Mach numbers approaching 20 with only minor engine geometry changes. At the lower limit of this envelope, the DMRJ operates in ramjet mode and combustion occurs at subsonic speeds. In this mode, the addition of heat can be used to drive the supersonic inflow to sonic conditions and achieve a thermal choke and a precombustion shock train forms in the DMRJ isolator. The shock train consists of a series of normal or oblique shocks, which terminate with a normal shock that drives the flow to subsonic conditions. The pre-combustion shock train aids flame stabilization by increasing the static pressure and temperature and decelerating the flow. In the dual-mode scramjet engine, a constant area diffuser (isolator) is placed upstream of the combustor to reduce the interaction of the combustor and intake flow field and to prevent the intake un-start. The position and strength of three-dimensional pre-combustion shock train and combustor heat release distribution are strongly coupled. However, as described in Heiser and Pratt (1994), at speeds approaching Mach 6, pressure losses associated with choking the flow increase and operational efficiency decreases. At M>6, the level of heat release may be reduced by flowpath geometry modification and/or reducing the fuel-flow rate. The DMRJ operates in scramjet mode, in which combustion occurs at supersonic speeds. Transition from subsonic to supersonic combustion is obtained by controlling the heat released due to combustion such that the thermal choke is alleviated. Once the heat release is reduced by a sufficient amount, the flow is no longer choked and the flow through the combustor remains largely supersonic. The schematic of flow field in DMRJ is shown in Figure 1.

The numerical simulation of this problem is highly challenging to CFD. This is due to (i) presence of large subsonic / supersonic flow field in the combustor/isolator, (ii) the related importance of high level of turbulence modeling necessary to predict the extent and shape of the interaction and (iii) downstream mixing and combustion at lower Mach number. Recent studies by Moon et al. (2000) have indicated a

pronounced effect of pre-combustion shock train and the level of predicted turbulent mixing on combustion. It has been shown that there exist two strong possibilities namely (1) strong turbulent mixing and (2) instability of shear layer between air and fuel jet as being mainly responsible for high thermal chocking. Debates are still going on in the current literature whether a simple H_2 –air kinetics can describe the overall features of the DMRJ operations or detailed kinetics is required to address the issues of mixing and combustion. Kanda et al. (2001) studied the dual mode operation in a Mach 2.5 air stream with total temperature and total pressure of 2000 K and 1.0 MPa respectively. They have achieved different modes of operation in the same combustor and at the same fuel flow rate by changing the fuel injection position. To validate CFD predictive capability, Goyne et al. (2002) studied both experimentally and numerically a simplified three dimensional combustor geometry in an electrically heated supersonic combustion facility (to get test gas free of contaminants). Numerical simulation carried out by White and Morrison (1999) using VULCAN code (a general purpose RANS solver with a wide variety of physical, thermo-chemical and turbulence models) under-predicted turbulent-air mixing and consequent lower heat release and the importance of accurate turbulence modeling is stressed. Dual-mode operation of the scramjet combustor was also investigated by Chinzei et al. (1993) at National Aerospace Laboratory (NAL, Sendai, Japan). Their experimental investigation in direct connect scramjet Combustor-Isolator rig has provided one of the very few important experimental data in the mid speed range.

The experimental studies of Chinzei et al. (1993) have been examined numerically by various research groups (McDaniel & Edwards, 2001; Salem et al., 2001, 2002; Mohieldin et al., 2001; Rodriguez et al., 2000) to understand the key features of upstream interaction and modeling of a dual-mode scramjet operation. McDaniel and Edwards (2001) simulated numerically the three dimensional flow field of DMRJ combustor using a low diffusion Flux Splitting Method (Edward, 1997) Mentor's SST model (Menter, 1994) and abridged SPARK model (Eklund et al., 1990) to study intake unstarting characteristics at different equivalence ratio. Salem et al. (2001) used Fluent Software (Fluent Inc., 1999) to study the flow field of the scramjet combustor and investigated the effect of initial boundary layer on the flow structure. Considerable upstream interaction was observed with the use of profile initial condition, where as the upstream interaction was not present with uniform initial condition. Mohieldin et al. (2001) reported asymmetry in the flow structure along with the random appearance of separation bubble and significant upstream interaction. Rodriguez et al. (2000) compared Various turbulence models namely, Menter's SST Model (Menter, 1994), Wilcox turbulence model (Wilcox, 1998) and Explicit Algebraic Stress model (Abid et al., 1995) for Chenzei's experimental case and all these models under-predicted the pressure values in the combustor. Appearance of massive sidewall separation bubble has also been reported in the simulation.

Although, several numerical simulations on this important experimental study have revealed many new aspects, the effect of incoming boundary layer on the flow development has not been addressed adequately. It is important to simulate the combustor flow field along with the facility nozzle so that proper boundary layer is accounted at combustor entry to predict the upstream interaction in dual mode combustion system. In this present work, dual-mode scramjet experimental study of Chinzei et al. (1993) is thermo-chemically explored to understand the effect of simple H_2-air kinetics and combustor entry boundary layer on upstream interaction using a commercial three dimensional reacting Navier Stokes solver CFX (ANSYS, Inc., 2004) along with k-ε turbulence model (Launder

&Spalding, 1974) Simulations were carried out from the throat of the facility nozzle, so that a realistic boundary layer is developed at the combustor entry. The computed surface pressure has been compared with the experimental values and the results of other numerical calculations and the flow parameters are analyzed to obtain the insight of the flow field in the combustor.

2. EXPERIMENTAL SET UP FOR WHICH THE COMPUTATIONS ARE CARRIED OUT

The schematic of the Dual-mode scramjet combustor experiment of Chinzei et al. (1993) for which the computations are carried out is shown in Figure 2. The combustor is essentially rectangular cross section of constant width with a duct length of 0.58 m. On both the upper and lower walls, there is a backward facing step of width 0.0032 m to contain combustion induced pressure rise. Further downstream, a 1.7^0 wall divergence is provided in order to maintain flow expansion and thus delay the formation of thermal choked condition. The addition of a constant area duct of height 0.032 m ahead of the combustor contains the upstream interaction without affecting the flow field in the facility nozzle. To simulate the proper boundary layer at the combustor entry, simulations are carried out from the throat of the facility nozzle. The vitiated air heater provides the inflow to the scramjet combustor through a Mach 2.5 facility nozzle at stagnation temperature and stagnation pressure of 2000 K and 1 MPa respectively. These conditions represent a flight condition corresponding to Mach 7.5. The oxygen, nitrogen and water vapor mass fraction of vitiated air are 0.24335, 0.5835 and 0.17315 respectively. Sonic Hydrogen at room temperature is injected in the combustor through nine injectors (five on bottom wall and four on the top wall) at an equivalence ratio of 0.8. The top injectors are interdigitated with respect to the bottom one to provide same flow rate from both the walls. A more detailed description of the experimental set up and test conditions are available in Ref 9.

3. ANALYSIS

3.1. Governing Equations

The appropriate system of equations governs the turbulent flow of a compressible gas may be written as

Continuity equation**:**

$$\frac{\partial \rho}{\partial t} + \frac{\partial}{\partial x_i}\left(\rho u_i\right) = 0 \ , i = 1,2,3 \tag{1}$$

Momentum equation **:**

$$\frac{\partial}{\partial t}\left(\rho u_i\right) + \frac{\partial}{\partial x_j}\left(\rho\ u_i u_j\right) + \frac{\partial P}{\partial x_i} = \frac{\partial(\tau_{ij})}{\partial x_j} \rho \sum_{k=1}^{ns} Y_k f_{k,j} \ , \quad i, j = 1,2,3 \tag{2}$$

Energy equation **:**

$$\frac{\partial}{\partial t}(\rho E) + \frac{\partial}{\partial x_i}(\rho u_i H) = \frac{\partial p}{\partial t} + \frac{\partial}{\partial x_j}\left(\tau_{ij} u_i\right) + \frac{\partial q_i}{\partial x_i} + \rho \sum_{k=1}^{ns} Y_k f_{k,i} u_i, \quad i,j = 1,2,3 \tag{3}$$

Turbulent kinetic energy (K) equation:

$$\frac{\partial}{\partial t}\left(\rho k\right) + \frac{\partial}{\partial x_i}\left(\rho u_i k\right) = \frac{\partial}{\partial x_i}\left(\left(\frac{\mu_l}{\mathrm{Pr}} + \frac{\mu_t}{\sigma_K}\right)\frac{\partial k}{\partial x_i}\right) + S_k \tag{4}$$

Rate of dissipation of turbulent kinetic energy (ε) equation:

$$\frac{\partial}{\partial t}\left(\rho \varepsilon\right) + \frac{\partial}{\partial x_k}\left(\rho u_k \varepsilon\right) = \frac{\partial}{\partial x_k}\left(\left(\frac{\mu_l}{\mathrm{Pr}} + \frac{\mu_t}{\sigma_\varepsilon}\right)\frac{\partial \varepsilon}{\partial x_k}\right) + S_\varepsilon \tag{5}$$

Species mass fraction (Y_i):

$$\frac{\partial}{\partial t}\left(\rho Y_i\right) + \frac{\partial}{\partial x_k}\left(\rho u_k Y_i\right) = \frac{\partial}{\partial x_k}\left(\left(\frac{\mu_l}{\mathrm{Pr}} + \frac{\mu_t}{\sigma_c}\right)\frac{\partial Y_i}{\partial x_k}\right) + \dot{w}_i \tag{6}$$

where, ρ, u_i, p, H, E, Y_i, $\dot{w}_i$ are the density, velocity components, pressure, total enthalpy, total energy species mass fraction and species production term respectively. $f_{k,i}$ is the body

Figure 2. Schematic of computational domain

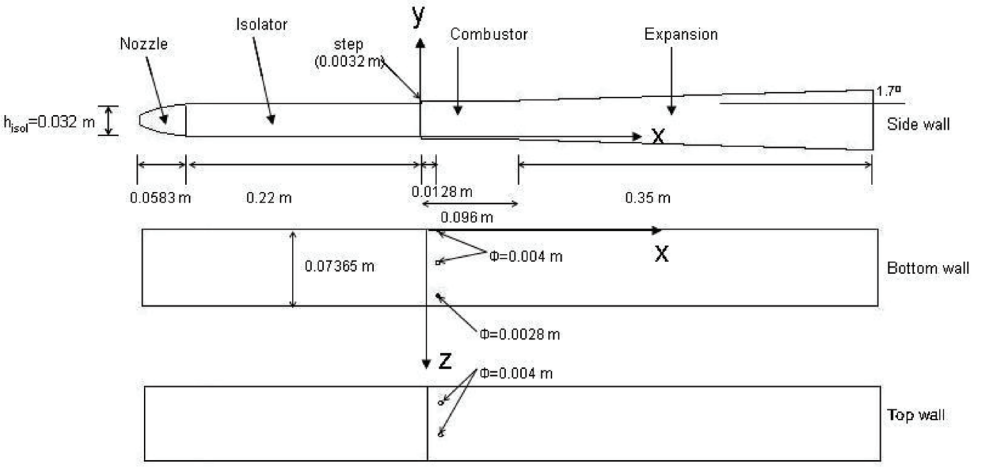

force the species k in the direction i and $\mu = \mu_l + \mu_t$ is the total viscosity; μ_l, μ_t being the laminar and turbulent viscosity and *Pr* is the Prandtl number. The source terms S_k and S_ε of the *K* and ε equation are defined as

$$S_k = \tau_{ij} \frac{\partial u_i}{\partial x_j} - \rho \varepsilon$$

and

$$S_\varepsilon = C_{\varepsilon 1} \tau_{ij} \frac{\partial u_i}{\partial x_j} - C_{\varepsilon 2} \frac{\rho \varepsilon^2}{k}$$

where, turbulent shear stress is defined as

$$\tau_{ik} = \mu_t \left(\frac{\partial u_i}{\partial x_k} + \frac{\partial u_k}{\partial x_i} \right) \quad (7)$$

Laminar viscosity (μ_l) is calculated from Sutherland law as

$$\mu_l = \mu_{ref} \left(\frac{T}{T_{ref}} \right)^{3/2} \left(\frac{T_{ref} + S}{T + S} \right) \quad (8)$$

where T is the temperature and μ_{ref}, T_{ref} and S are known coefficients. The turbulent viscosity μ_t is calculated as

$$\mu_t = c_\mu \frac{\rho k^2}{\varepsilon} \quad (9)$$

The coefficients involved in the calculation of μ_t are taken as

c_μ =0.09, $C_{\varepsilon 1}$=1.44, $C_{\varepsilon 2}$ = 1.92

σ_K =1.0, σ_ε =1.3, σ_c = 0.9

The heat flux q_k is calculated as $q_k = -\lambda \frac{\partial T}{\partial x_k}$, λ is the thermal conductivity.

3.2. Combustion Modeling

The Eddy Dissipation Concept (EDC) based combustion model is used for the simulation. The EDC combustion model, used extensively for its simplicity and robustness in predicting reactive flows, is based on the concept that chemical reaction is very fast relative to the

transport process in the flow. The products are formed instantaneously as the reactants mix at the molecular level. The model assumes that the reaction rate may be related directly to the time required to mix reactants at molecular level. In turbulent flows, this mixing time is dictated by the eddy properties and therefore, the burning rate in proportional to the rate at which turbulent kinetic energy is dissipated i.e., reaction rate is proportional to ε/k. The chemistry of the combustion reaction of hydrogen in air is represented on a molar basis by: $H_2 + ½\ O_2 = H_2O$.

3.3. Discretization of Governing Equations

Hybrid grid is used in the simulation. The grid is structured (hexahedral elements) with fine meshing (about 20 layers) near the walls to capture the wall boundary layer and unstructured (tetrahedral element) in the rest of the domain. A total number of 0.43 million nodes are employed in the computational domain. The grid is adequate to capture the essential feature of the flow field as shown through the grid independence of the results (presented later).

The CFX-TASC flow solver utilizes a finite volume approach, in which the conservation equations in differential form are integrated over a control volume described around a node, to obtain an integral equation. The pressure integral terms in the momentum integral equation and the spatial derivative terms in the integral equations are evaluated using finite element approach. The convective terms are evaluated using a second order upwind differencing with physical advection correction and central differencing is used to discretize viscous terms. The set of discretized equations form a set of algebraic equations: $A\ \vec{x} = b$ where, $\vec{x}$ is the solution vector. The solver uses an iterative procedure to update an approximated x_n (solution of x at n^{th} time level) by solving for an approximate correction x' from the equation $A\ \vec{x'} = \vec{R}$, where $\vec{R} = \vec{b} - A\vec{x}_n$ is the residual at n^{th} time level. The set of non-linear algebraic equations $A\ \vec{x'} = \vec{R}$ is solved iteratively using Lower Upper factorization method. An algebraic multigrid method is implemented to reduce low frequency errors in the solution of the algebraic equations. Maximum residual $(= \varphi_j^{n+1} - f\left(\varphi_j^{n+1}, \varphi_j^n\right)) < 10^{-4}$ is taken as convergence criteria.

4. RESULTS AND DISCUSSIONS

As mentioned earlier, the computational domain starts from the throat of the facility nozzle, so that the boundary layer at the combustor entry is captured accurately. Taking the advantage of the symmetry of the combustor geometry, only

Figure 3. Grid distribution in (a) symmetry plane and (b) plane passing through all injectors

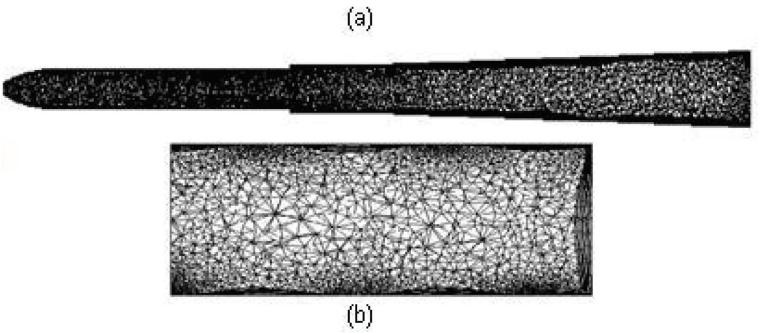

Figure 4. Side wall pressure distribution for two different grid structures

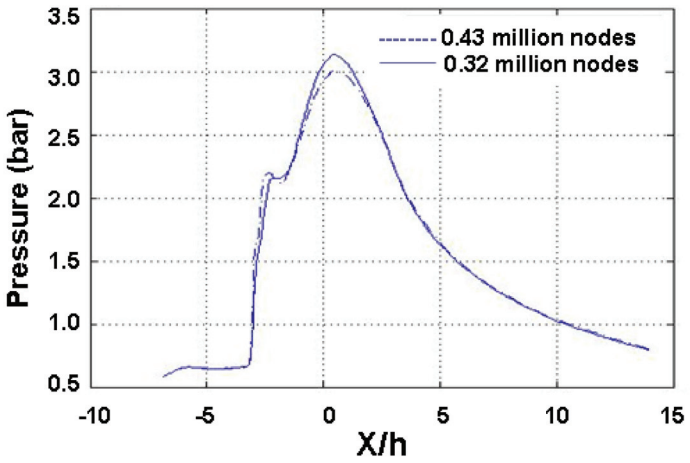

one half of the geometry is simulated. Typical grid distribution in the symmetry plane and in the cross sectional plane passing through all the injectors is shown in Figure 3. In the simulation, X axis is taken along the length of the combustor, while Y and Z axis are taken along the height and width of the combustor. The location of the step at the plane of symmetry is taken as the origin. The inflow conditions of the Hydrogen and air stream used in the simulation are tabulated in Table 1

As the computational domain starts from the throat of the facility nozzle, sonic condition along with the total temperature and total pressure of 2000 K and 1 MPa is applied in the inflow plane. No slip and adiabatic wall boundary conditions are imposed at the solid wall, while the supersonic outflow boundary conditions are applied at the outflow boundary. Scalable wall function is employed for turbulence quantities at the combustor wall and 10% turbulence intensity is prescribed at the inflow plane.

The grid independence of the solution is established by carrying out the calculation with a grid distribution of 0.32 million nodes and comparing the wall pressures at the top surface between the two grids in Figure 4. It is very clear from the figure that by changing the grids from 0.43 to 0.32 million, the peak pressure changes by about 6%. Although, further grid refinement studies have not been undertaken; the present grid is considered adequate to capture the essential features of the solutions.

The qualitative features of the flow field are depicted through the comparison of various thermochemical parameters for reacting and non-reacting cases in Figures 5 through 8. The

Table 1. Inflow conditions of the air stream and the hydrogen jet

Parameters	Air	Hydrogen
Mach number	2.5	1.0
Static temperature (K)	2000	300
O_2 mass fraction	0.24335	0.0
H_2O mass fraction	0.17315	0.0
N_2 mass fraction	0.5835	0.0
H_2 mass fraction	0.0	1.0

Figure 5. Mach No. distribution in the plane of symmetry

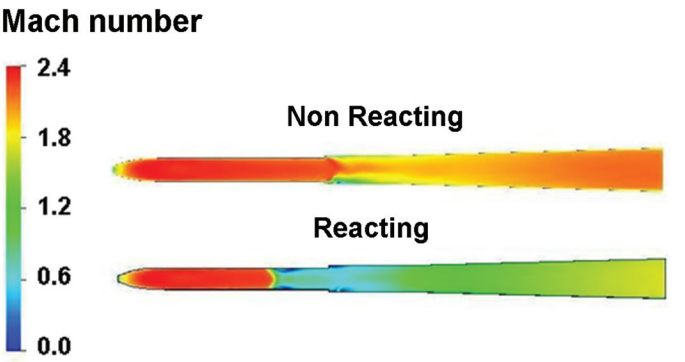

Figure 6. Pressure distribution in the plane of symmetry

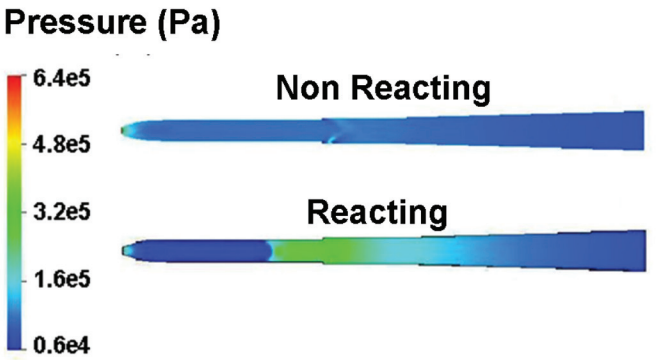

Figure 7. Water mass fraction and Temperature distribution in the plane of symmetry

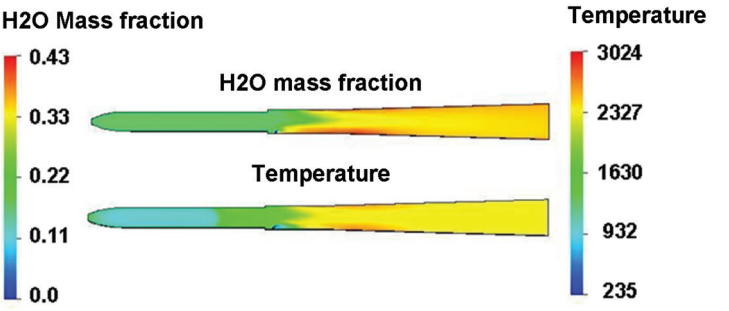

Figure 8. Y_{H2o} distribution at different axial locations (x/h = -4.26, -0.89, 0.68, 3.8, 6.93 and 11.62)

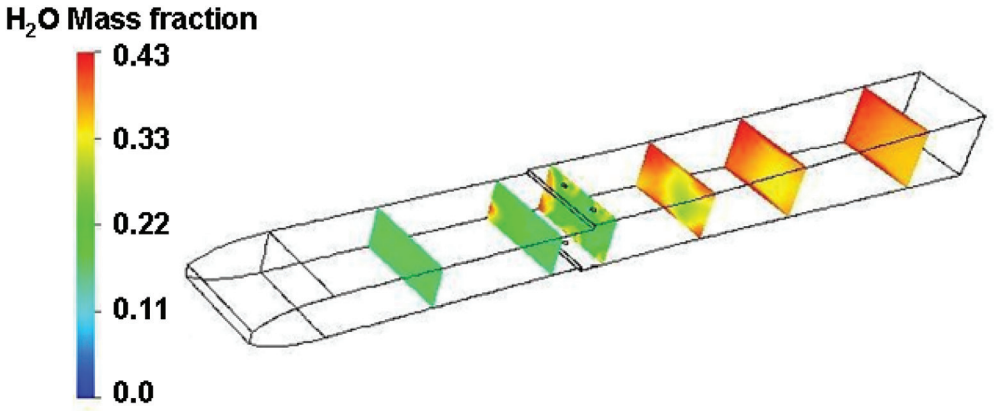

Mach number distributions in the plane of symmetry between the reacting and non-reacting cases are shown in Figure 5. For the reacting case, a normal shock is seen to occur at X/h = -2.8 (where h = 0.032m is the height of the isolator), while the flow field is seen to be completely supersonic in the non-reacting case. The heat release due to reaction is responsible for this upstream condition. The low speed recirculation at the backward facing step and the flow expansion at the divergent portion of the combustor are clearly visible in the figure.

The same feature of upstream interaction due to heat release is also clearly seen in the comparison of pressure distribution in the symmetry plane between reacting and non-reacting cases presented in Figure 6. The water mass fraction and temperature distribution present in Figure 7 in the plane of symmetry depicts the zone – covered by the reaction products. It is observed that from x/h = 4.0, the entire cross section is filled with the water vapor. The cross sectional view of water vapor mass fraction distribution at x/h = -4.26, -0.89, 0.68, 3.8, 6.93

Figure 9. Y_{H2} distribution at different axial locations (x/h =-2.76, -1.2 and 0.4)

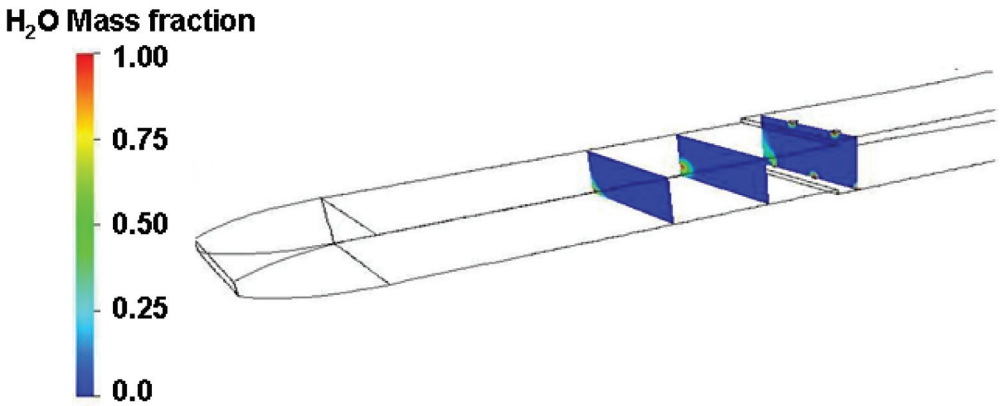

Figure 10. U-velocity distribution at different axial locations (x/h = -2.8, -1.5, -.26 and 1.02)

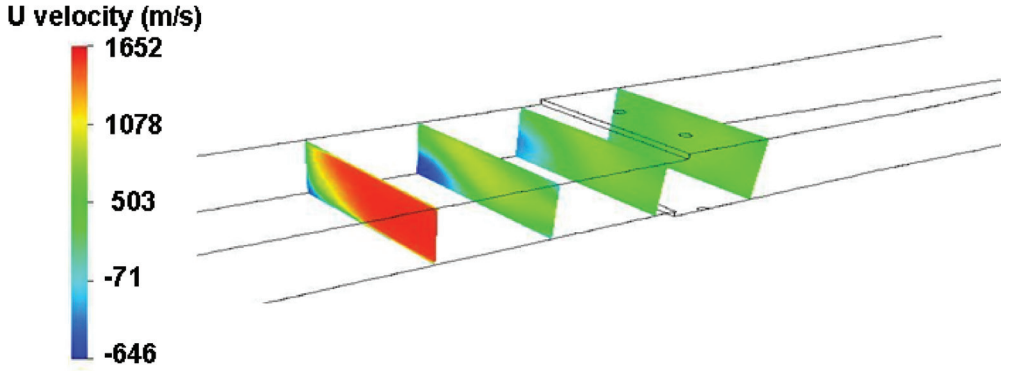

and 11.62 shown in Figure 8 clearly depicts the development of reaction zone along the length of the combustor. Hydrogen mass fraction at x/h = -2.76, -1.2 and 0.4 is presented in Figure 9. Although the Hydrogen is injected perpendicularly at x/h = 0.4, it has diffused upstream up to x/h = -2.76 through the sidewall separation bubble. A massive separation bubble is seen to occur at the sidewall due to heat release as shown through the cross sectional view of the velocity vector plot at x/h = -2.8, -1.5, -.26 and 1.02 presented in Figure 10. Massive sidewall separation is also observed in the simulation of Mohieldin et al. (2001) with profile boundary condition. The length of the sidewall separation bubble is about 3h.

The axial distribution of the computed surface pressure on the sidewall is compared with the experimental data (Chinzei et al., 1993) and the numerical results of VULCAN code (Rodriguez et al., 2000) in Figure 10. Also, presented in the figure, is the surface pressure obtained from the nonreacting simulation. Reasonable agreement has been obtained be-

Figure 11. Comparison of side wall surface pressure distribution

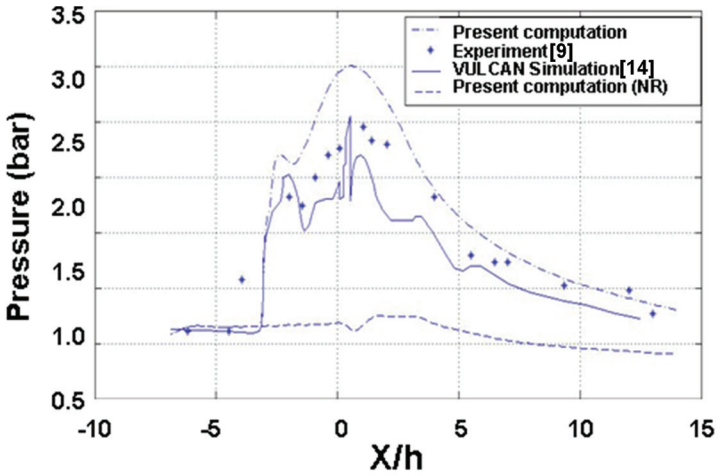

Figure 12. Comparison of bottom wall surface pressure distribution

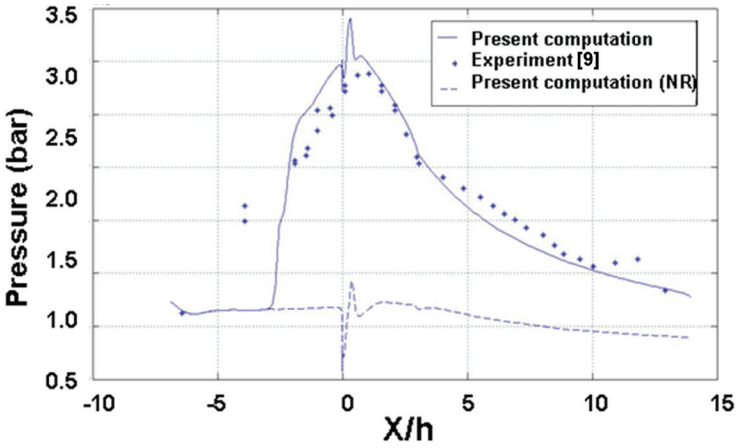

tween experimental and computed values. Present computations over-predict the surface pressure particularly in the zone of injection, while VULCAN code under-predicts the surface pressure. Higher heat release caused due to use of fast chemistry to model combustion is perhaps responsible to obtain higher surface pressure in the present computation. In the divergent section of the combustor (the thrust producing element in the combustor), the present prediction matches better with the experimental results compared to the VULCAN simulation (Rodriguez et al., 2000). It is to be noted that abridged SPARK model (Eklund et al., 1990) containing seven steps, seven species finite rate chemical kinetics is used in VULCAN code in the present problem. Both the numerical results predict the location of normal shock (upstream interaction) at 0.5 h downstream compared to the experimental values. The difference of pressure between reacting and non-reacting cases quantifies the pressure rise due to heat release. This

Figure 13. Comparison of surface pressure distribution between three walls

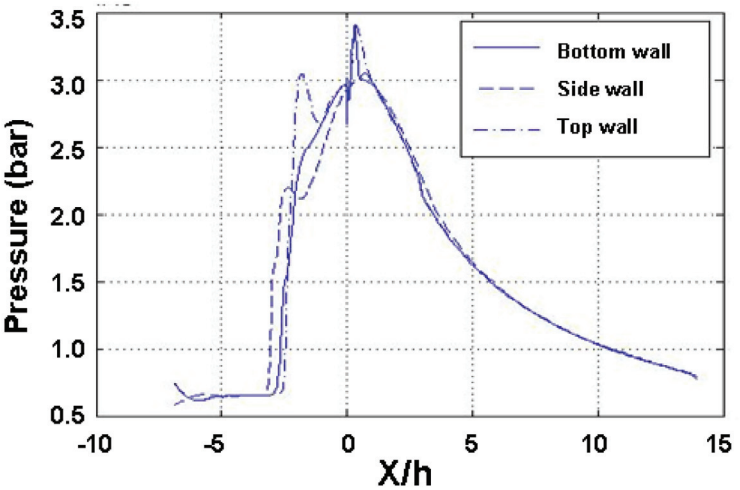

Figure 14. Mach No distribution in the plane of symmetry for with and without facility nozzle

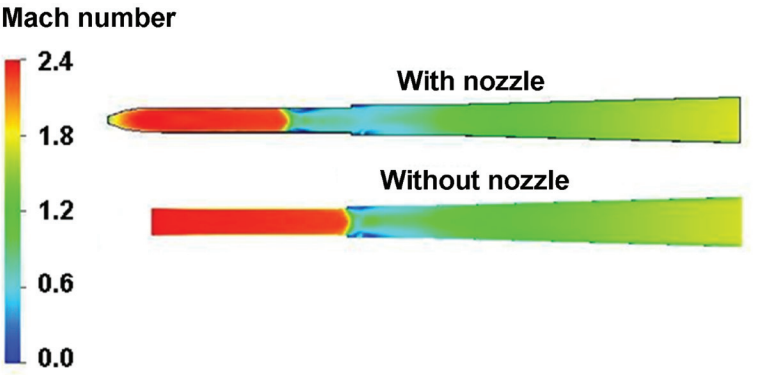

comparison demonstrates that a simple H_2-air kinetics may be adequate to predict the overall features of hydrogen combustion in DMRJ combustor. The numerical models need to be fine tuned to predict correctly the upstream interaction point. The comparison of the side wall pressure distribution with experimental value is presented in Figure 11. The comparison of bottom wall pressure distribution with experimental value is presented in Figure 12. Reasonable match is observed although the prediction shows slightly higher value due to the use of fast chemistry as stated earlier. The axial distribution of the surface pressure at the bottom, top and sidewall is compared in Figure 13. The differences of surface pressure in the upstream region is due to the sidewall separation and the values merge into one from x/h=3 onwards.

Simulation was also carried out without the facility nozzle and imposing the uniform flow condition corresponding to Mach 2.5 at the combustor entry to determine the effect of incoming boundary layer in the flow develop-

Figure 15. Comparison of sidewall pressure distribution in the plane of symmetry for with and without facility nozzle

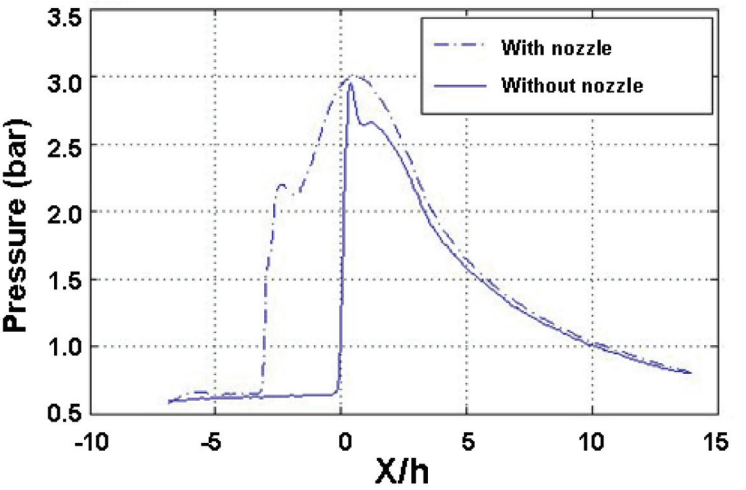

Figure 16. Axial distribution of combustion efficiency

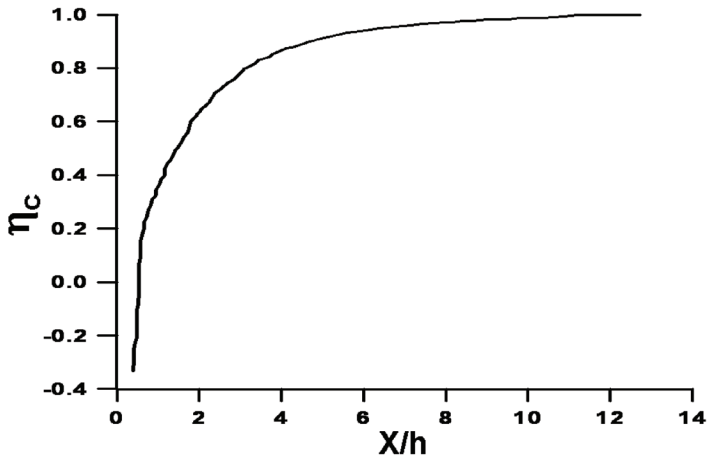

ment in the combustor. The Mach number distributions in the plane of symmetry between the two cases are set out in Figure 14. The simulation with facility nozzle shows significant upstream interaction compared to the simulation with uniform condition at the combustor entry. The boundary layer at the combustor entry present in the simulation with facility nozzle is mainly responsible for this upstream interaction. The effect of upstream interaction with the boundary layer at combustor entry is very starkly visible in the comparison of the surface pressures on the sidewall for these two cases in Figure 15. These results demonstrate the importance of considering proper boundary layer in the flow characteristics in the scramjet combustor. The axial distribution of combustion efficiency is defined as

$$\eta_C = \int (\rho u Y_{H2} \partial A) / \dot{m}_{H2}$$

(where $\dot{m}_{H2}$ and Y_{H2} the mass flow rate and mass fraction of hydrogen respectively) is shown in Figure 16. Reaction is seen to be completed at x/h = 12.

5. CONCLUSION

Numerical simulation is presented to understand the key features of upstream interaction, mixing and combustion in dual mode scramjet engine. Three dimensional Navier Stokes equations along with K-∈ turbulence model and Eddy Dissipation Concept (EDC) based combustion model are solved using commercial CFD Software. To get realistic boundary layer profile at the combustor entry, flow field is simulated from the throat of the facility nozzle. Computed surface pressure matches reasonably well with the experimental results and the results of other numerical computations. The computation overpredicts the surface pressure particularly in the zone of injection because of higher heat release due to fast chemistry assumption in combustion modeling, but in the divergent section (where the major portion of thrust is produced), the computation predicts the experimental results quiet well. The computed position of normal shock (upstream interaction point) is at downstream location compared to experimental result. It has been demonstrated that simple kinetics and turbulence – chemistry interaction model may be adequate to address the overall flow features in the combustor. The

boundary layer of the incoming air stream of the combustor entry is shown to have a pronounced effect and cause significant upstream interaction compared to the uniform flow at the combustor entry. The reaction zone is seen to cover the whole combustor cross section and reaction is seen to proceed to completion. The simulation has helped immensely in understanding the complex flow pattern inside the engine.

REFERENCES

Abdel Salem, T. M., Tiwari, S. N., & Mohieldin, T. O. (2001). *Dual mode flow field in scramjet combustor (AIAA Paper No. 2001 – 2966)*. Reston, VA: American Institute of Aeronautics and Astronautics.

Abdel Salem, T. M., Tiwari, S. N., & Mohieldin, T. O. (2002). *Three dimensional numerical study of a scramjet combustor (AIAA Paper No. 2002 – 0805)*. Reston, VA: American Institute of Aeronautics and Astronautics.

Abid, R., Rumsey, C. L., Gatski, T. B., & Speziale, C. G. (1995). Prediction of non equilibrium turbulent flows with explicit algebraic turbulence models. *AIAA Journal*, *33*(11). doi:10.2514/3.12943

ANSYS, Inc. (2004). *CFX 5.7: Computational fluid dynamics software*. Canonsburg, PA: Author.

Billig, F. S. (1993). Research on supersonic combustion. *Journal of Propulsion and Power*, *9*(4), 499–514. doi:10.2514/3.23652

Chinzei, N., Komuro, T., Kudou, K., Murakami, A., Tassi, K., Masuya, G., & Wakamatou, Y. (1993). Effects of injector geometry on Scramjet combustor performance. *Journal of Propulsion and Power*, *9*(1), 146–152. doi:10.2514/3.11497

Cockrell, C. E. Jr, Auslender, A. H., Guy, R. W., McClinton, C. R., & Welch, S. S. (2002). *Technology roadmap for dual-mode scramjet propulsion to support space-access vision vehicle development (AIAA Paper No. 2002-5188)*. Reston, VA: American Institute of Aeronautics and Astronautics.

Curran, E. T. (2001). Scramjet engine: The first forty years. *Journal of Propulsion and Power*, *17*(6), 1138–1148. doi:10.2514/2.5875

Edwards, J. R. (1997). A low-diffusion flux-splitting scheme for Navier-stokes calculation. *Computers & Fluids*, *26*(6), 635–659. doi:10.1016/S0045-7930(97)00014-5

Eklund, D. R., Drummond, J. P., & Hassan, H. A. (1990). Calculation of supersonic turbulent reacting co-axial jets. *AIAA Journal*, *28*, 1633–1641. doi:10.2514/3.25262

Fluent, Inc. (1999). *Fluent version 5 user guide*. New York, NY: Author.

Goyne, C. P., Rodriguez, C. Z., Krauss, R. H., McDaniel, J. C., & McClinton, C. R. (2002). *Experimental and numerical study of a duct mode scramjet combustor (AIAA Paper No. 2002 – 5216)*. Reston, VA: American Institute of Aeronautics and Astronautics.

Heiser, W. H., & Pratt, D. T. (1994). *Hypersonic airbreathing propulsion (AIAA Education Series)*. Reston, VA: American Institute of Aeronautics and Astronautics.

Kanda, T., Chinzei, N., Kudo, K., & Murakami, A. (2001). *Dual mode operation in a scramjet combustor (AIAA Paper No. 2001 – 1816)*. Reston, VA: American Institute of Aeronautics and Astronautics.

Launder, B. E., & Spalding, D. B. (1974). The numerical computation of turbulent flows. *Computer Methods in Applied Mechanics and Engineering*, *3*, 269–289. doi:10.1016/0045-7825(74)90029-2

McDaniel, K. S., & Edwards, J. R. (2001). *Three dimensional simulation of thermal chocking in a model scramjet combustor (AIAA Paper No. 2001 – 0382)*. Reston, VA: American Institute of Aeronautics and Astronautics.

Menter, F. R. (1994). Two-equation eddy – Viscosity turbulence models for engineering applications. *AIAA Journal*, *32*(8), 1598–1605. doi:10.2514/3.12149

Mohieldin, T. O., Tiwari, S. N., & Olyneiw, M. J. (2001). *Asymmetric flow structures in dual mode scramjet combustor with significant upstream interaction (AIAA Paper No. 2001 – 3296)*. Reston, VA: American Institute of Aeronautics and Astronautics.

Moon, G. W., Jeung, I. S., & Choi, J. Y. (2000). *Numerical study of thermal choking process in a model scramjet engine (AIAA Paper No. 2000-3706)*. Reston, VA: American Institute of Aeronautics and Astronautics.

Rodriguez, C. G., White, J. A., & Riggins, D. W. (2000). *Three dimensional effects in modeling dual mode scramjets (AIAA Paper No. 2000 – 3704)*. Reston, VA: American Institute of Aeronautics and Astronautics.

White, J. A., & Morrison, J. H. (1999). *A pseudo temporal multigrid relaxation scheme for solving the parabolized Navier Stokes equations (AIAA Paper No. 1999 – 3360)*. Reston, VA: American Institute of Aeronautics and Astronautics.

Wilcox, D. C. (1998). *Turbulence modeling for CFD. La Canada Flintridge*. CA: DCW Industries.

Rahul Inlge holds a master degree in mechanical engineering from Indian Institute of Science, Bangalore, India. He has a more than 7 years of experience in computational fluid dynamics area with good understanding of modeling compressible multiphase and reacting flow. At present he is working at ANSYS Fluent India Pvt Ltd as a Senior Technology Specialist. Before joining ANSYS he worked at Defense Research Development Laboratory (DRDL), Hyderabad, India, as a scientist where he contributed mainly in design and development of missile propulsion system. This work was carried out when he was working at DRDL.

Debasis Chakraborty obtained his PhD in Aerospace Engineering from Indian Institute of Science (IISc), Bengaluru, India. Presently, he is working as Technology Director, Computational Dynamics Directorate, at Defense Research and Development Laboratory (DRDL), Hyderabad, India. His research interests are CFD, aerodynamics, high-speed combustion, and propulsion. He has about 35 journal and 50 conference publications to his credit.